

- ¹⁵R. Moreh, D. Salzmann, and Y. Wand, *Phys. Letters* **30B**, 536 (1969).
- ¹⁶M. Ferentz and N. Rosenzweig, in *Alpha-, Beta-, and Gamma-Ray Spectroscopy*, edited by K. Siegbahn (North-Holland Publishing Company, Amsterdam, The Netherlands, 1966), p. 1687.
- ¹⁷L. C. Biedenharn and M. E. Rose, *Rev. Mod. Phys.* **25**, 729 (1953).
- ¹⁸L. W. Fagg and S. S. Hanna, *Rev. Mod. Phys.* **31**, 711 (1959).
- ¹⁹F. Metzger and M. Deutsch, *Phys. Rev.* **78**, 551 (1950).
- ²⁰R. Moreh and M. Friedman, *Phys. Letters* **26B**, 579 (1968). This article contains an error. The role of $E1$ and $M1$ transitions was reversed; thus the transitions from the resonance level in ^{62}Ni and ^{112}Cd are $E1$, while those in ^{141}Pr and ^{208}Pb are $M1$.
- ²¹G. A. Bartholomew, M. R. Gunye, and E. D. Earle, *Can. J. Phys.* **45**, 2063 (1967).
- ²²L. M. Bollinger, in *Nuclear Spectroscopy*, edited by F. Ajzenberg-Selove (Academic Press Inc., New York, 1960), Part A, p. 417.
- ²³J. Julien *et al.*, *Nucl. Phys.* **A132**, 129 (1969).
- ²⁴C. E. Porter and R. G. Thomas, *Phys. Rev.* **104**, 483 (1956).
- ²⁵K. Reibel and A. K. Mann, *Phys. Rev.* **118**, 701 (1960).
- ²⁶P. Axel, *Phys. Rev.* **126**, 671 (1962).
- ²⁷E. G. Fuller and E. Hayward, in *Nuclear Reactions*, edited by P. M. Endt and P. B. Smith (North-Holland Publishing Company, Amsterdam, The Netherlands, 1962), Vol. II, pp. 189–190.
- ²⁸R. Moreh and A. Wolf, to be published.
- ²⁹J. A. Harvey and G. G. Slaughter, Oak Ridge National Laboratory Report No. ORNL 3924, 1966 (unpublished), p. 28.
- ³⁰G. A. Bartholomew, *Ann. Rev. Nucl. Sci.* **11**, 259 (1961).
- ³¹L. M. Bollinger, in *International Symposium on Nuclear Structure, Dubna, 1968* (International Atomic Energy Agency, Vienna, Austria, 1969), p. 317.
- ³²J. A. Biggerstaff, J. R. Bird, J. H. Gibbons, and W. M. Good, *Phys. Rev.* **154**, 1136 (1967).

Neutron Emission in Alpha-Particle-Accompanied Fission

Eran Nardi

Israel Atomic Energy Commission Soreq Research Center, Yavne, Israel and Weizmann Institute of Science, Rehovot, Israel

and

Zeev Fraenkel

Weizmann Institute of Science, Rehovot, Israel

(Received 6 April 1970)

A four-parameter correlation experiment which measured neutron emission in "long-range alpha" (LRA) fission is described. The energies of both the fission fragments and of the α particle as well as the time of flight of the neutron were recorded. The experimental data were analyzed with the aid of a computer, and the method of analysis is described.

Some of the results of the present experiment have already been published. In this paper we discuss the pre-neutron-emission mass distribution of LRA fission as well as some properties of the neutrons as a function of α -particle energy. In addition, the neutron kinetic energy as a function of fragment mass is given. The probability of α -particle emission as a function of the fission-fragment mass ratio is also discussed.

I. INTRODUCTION

At present there are two principal methods for studying the scission configuration of a fissioning nucleus. The first method is to investigate the properties of the prompt neutrons emitted from individual fission fragments, thereby obtaining information on the deformation energies of the various fission fragments at scission. These studies were summarized by Terrell.¹ The most important characteristic of the prompt neutrons in low-energy fission is the "saw tooth" dependence of the average number of neutrons as a function of frag-

ment mass. The second method of obtaining information on the point of scission is by studying the properties of the α particles and fission fragments in "long-range alpha" fission (LRA fission). This process, which occurs about once in every 300 fission events, is characterized by the emission of an α particle in addition to the fission fragments. As has been discussed by Halpern² and by Fraenkel,³ the fact that the α particle seems to be emitted at or very near the time of scission makes this particle extremely useful in studying the initial conditions at scission. The main conclusion obtained in studying the LRA fission process is

that at the point of scission the fragments are already moving with a substantial part of their final kinetic energy.^{2,4}

A most important question which arises in connection with LRA fission is whether its scission configuration is essentially the same as that of binary fission. In order to resolve this problem, a comparison of the properties of scission in binary and LRA fission must be made. A prominent property of the scission configuration is the average number of neutrons as a function of fragment mass, since it gives the variation of the fragment deformation energy at the moment of scission as a function of fragment mass. The main motivation in carrying out the present experiment was to clarify the question of the similarity of the scission properties of binary and LRA fission. In this experiment we compared the properties of the prompt neutrons in binary and LRA fission for the spontaneous fission of ²⁵²Cf.

In a previous publication,⁵ some results obtained in the present experiment were presented. The average number of neutrons as a function of fragment mass in LRA fission was found to be very nearly equal to that in binary fission [see Fig. 2(a) of Ref. 5]. This result will be discussed here in greater detail.

II. EXPERIMENTAL METHOD

A. Experimental Arrangement and Electronic Block Diagram

A schematic representation of the experiment, together with the block diagram of the electronics, are shown in Fig. 1. A ²⁵²Cf source of $\sim 2 \times 10^5$ fission/min, situated on a thin Ni backing was placed in the center of the vacuum chamber. Inside the vacuum chamber were also four solid-state counters, two fission counters designated by *F1* and *F2*, and two α -particle counters, $\alpha 1$ and $\alpha 2$. Gold foils of 17 mg/cm² were placed in front of each α counter in order to prevent fission fragments and the 6.1-MeV α particles from the radioactive decay of ²⁵²Cf from reaching the solid-state counters. The vacuum chamber was made of aluminum and had a diameter of 30 cm and a wall thickness of 5 mm. The two identical neutron detectors were placed opposite each other outside the vacuum chamber at a distance of 30 cm from the source and along the fission detector axis. The neutron detectors were NE102A plastic scintillators of 5-in. diameter and 10-cm depth mounted on 58 AVP photomultipliers. The neutron energy was determined by the time-of-flight method.

The angles subtended by the detectors in the vacuum chamber relative to the source were large. For the fission-fragment detectors this angle was

44° for each detector, while for the α counters the angle subtended by each detector was 60°. The neutron flight path of 30 cm was also relatively short compared with the depth of the scintillator. This experimental geometry was chosen in order to obtain a reasonable counting rate, since the experimental information of interest was obtained from the fourfold coincidence data of the relatively rare LRA-fission events. But the large angular apertures, the short flight path, and the substantial length of the scintillator introduced appreciable dispersion in the data.

The events were fed into a four-dimensional analyzer. They consisted of the following pulses: *F1* and *F2*, the pulse heights from both fission fragment detectors, TAC (time-to-amplitude converter) – the pulse proportional to the time difference between the start signal furnished by solid-state counter *F1* and the stop signal obtained by the interaction of the neutrons or γ rays with one of the scintillators. The fourth pulse was the α -particle pulse height which was obtained from either detector $\alpha 1$ or detector $\alpha 2$. The separation of TAC pulses originating from photomultipliers PM1 and PM2 was accomplished by routing the TAC pulses, while the $\alpha 1$ and $\alpha 2$ were separated by routing the α pulses to different parts of the analyzer memory. The number of channels in each dimension of the analyzer was 512.

In addition to the above-mentioned pulses, a gate pulse was also fed into the analyzer (see Fig. 1). This pulse determined what type of experimental data was being recorded. The main coincidence circuit was set during most of the experiment to the coincidence requirement $F1 \cap F2 \cap \alpha$. In these experiments we also recorded the four-dimensional events $F1 \cap F2 \cap \alpha \cap TAC$ which constituted the new experimental results obtained here. In addition, experiments with the coincidence requirements $F1 \cap F2$ and $F1 \cap F2 \cap TAC$ were also carried out. The data from the latter two experiments were used both for obtaining binary-fission data and for calibrations. All experimental data obtained here were stored on magnetic tape and were analyzed with the aid of a computer. The timing pulse from each photomultiplier was obtained by feeding the anode pulse to a fast trigger unit. The *F1* trigger output pulse was fed together with the fast photomultiplier pulse into an AND circuit, the output signal of which was proportional to the measure of overlap of both input pulses. In this manner the TAC pulse was generated. The cut-off energies of each of the photomultiplier trigger units were adjusted to correspond to a neutron kinetic energy of 250 keV. The lower-level discriminator of the α -particle detector was set at 11.5 MeV, because of the high rate

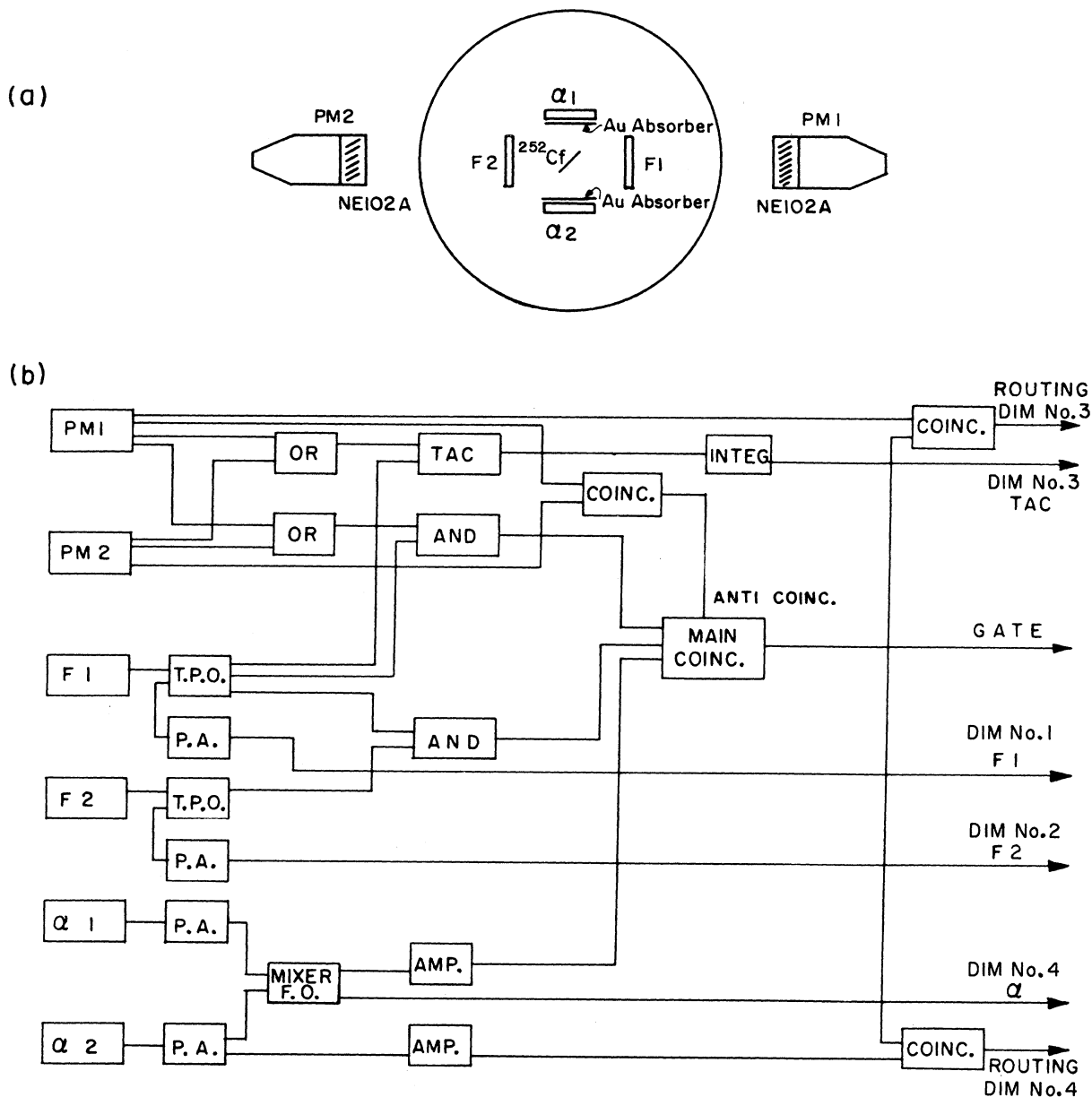


FIG. 1. Schematic representation of (a) experimental arrangement and (b) block diagram.
(T.P.O.—time pickoff unit.)

of the 6.1-MeV α particles from the decay of ^{252}Cf .

B. Data Collection

A total of 8500 LRA-fission neutrons in coincidence with both fission fragments and with the α particle were recorded. In addition a total of about 650 000 binary-fission neutrons coincident with both fission fragments were obtained from the experiments of the type $F1 \cap F2 \cap \text{TAC}$. The experiment was carried out for a period of 90 days,

and the solid-state counters and TAC system were checked every 24 h.

III. ANALYSIS OF THE DATA

The main purpose of the experiment was to obtain the average number of neutrons $\bar{\nu}$, both as a function of the mass of the fission fragment A , and as a function of the total kinetic energy of both fission fragments, E_F .

The following discussion will be devoted mainly

to the method with which $\bar{\nu}$ was obtained on the basis of the four correlated experimental quantities E_1 , E_2 , T , and E_α which denote, respectively, the energies of both fission fragments, the time of flight of the neutron, and the energy of the α particle. However, in order to obtain $\bar{\nu}$ the values of both A and E_F had to be determined.

A. Determination of the Energy and Mass of the Fission Fragment

The energy calibration of the fission-fragment detectors was carried out by assuming a simple linear dependence of the energy E on the pulse height x , i.e., $E = ax + b$. The more accurate calibration method of Schmitt, Kiker, and Williams⁶ was not used here since the high rate of fission fragments incident on the counters (of about 10^7 fragments per day) caused appreciable radiation damage, which increased with time. In this case, the behavior of the calibration parameters given by Schmitt, Kiker, and Williams⁶ are unknown, and for lack of better information we assumed the simple linear dependence.

The calibration constants a and b were obtained from the positions of the light and heavy peaks of the single-fragment kinetic-energy spectrum of the fission fragments in binary fission. The positions of the peaks were determined by fitting each peak to a Gaussian, using a least-squares method. The calibration energies were taken from the time-of-flight data of Whetstone⁷ corrected for neutron emission. The energies of the heavy and light peaks thus obtained were 79.55 and 104.3 MeV, respectively.

The method used here in obtaining the pre-neutron-emission mass distribution from the measured fission-fragment kinetic energies when the values of the average number of neutrons as a function of fragment mass are known is due to Schmitt, Neiler, and Walter.⁸ However, in LRA fission the situation is somewhat complicated as a result of the emission of the α particle. In formulating the equation of conservation of momentum of the fission fragments, we must also account for the recoil of the fission fragments as a result of α emission. This problem has been dealt with by Fraenkel³ who derived the relation between the energy ratio and mass ratio. If θ_L denotes the measured angle of the α particle with respect to the direction of the light fragment, this relation is given by

$$\frac{E'_L}{E'_H} \approx \frac{m'_H}{m'_L} \left[1 - \left(\frac{m_\alpha E_\alpha}{m'_H E'_H} \right)^{1/2} \cos \theta_L \right]^2. \quad (1)$$

The subscripts H and L denote the heavy and light

fragments, respectively, and m_α and E_α the mass and energy of the α particle. The values of E'_L , E'_H , m'_H , and m'_L are pre-neutron-emission quantities which were obtained using the method of Schmitt, Neiler, and Walter.⁸

B. Analysis of the Neutron Data

The first step in analyzing the neutron data was to obtain from the experimental TAC event the time of flight T of the neutron, and the kinetic energy of the neutron in the lab system. The position of the γ peak was found to shift in an essentially linear manner as a function of the mass of the fission fragment which triggered the start signal. The maximum shift from lightest to heaviest fragment was 0.5 nsec, and this effect was corrected for.

The sources of uncertainty in obtaining T are discussed in the Appendix. They are mainly due to the large uncertainty in the length of the neutron flight path as a result of the relatively large depth of the scintillator, and are also due to the experimental resolution in determining the time-of-flight value. The latter quantity is given by the standard deviation of the prompt γ peak of the time-of-flight spectrum, which was equal to 1.5 nsec. We denote the standard deviation of the error in the measurement of T by ΔT (see Appendix), and the standard deviation of the neutron time-of-flight spectrum by σ_T . A dispersion correction⁹ for each experimental time-of-flight value was carried out by shifting each experimental point by $[\Delta T^2 / (\sigma_T^2 + \Delta T^2)]^{1/2}$ in the direction of the average time-of-flight value.

The properties of the neutrons were studied by observing the neutrons emitted in the direction of motion of the fission fragments. The analysis of the neutron data was based on the hypothesis that *the neutrons are emitted isotropically in the c.m. system from fully accelerated fission fragments*. The experimental results obtained for the binary fission of ²⁵²Cf by Bowman *et al.*⁹ indicate that approximately 90% of the neutrons can be accounted for on the basis of this hypothesis. In a previous publication⁵ it was seen that the results of this experiment indicate that the properties of the neutrons in LRA fission closely resemble those of binary fission. In addition, Piekartz *et al.*¹⁰ observed that the angular distribution of the neutrons in the LRA fission of ²⁵²Cf is essentially equal to that in binary fission. Hence we can conclude that the isotropic-evaporation hypothesis is also valid in LRA fission. On the basis of this hypothesis it can be shown that the neutrons emitted from fragments incident on detector $F1$ (Fig. 1) are almost exclusively detected by the photomultiplier $PM1$,

while those emitted from fragments striking $F2$ are detected only by PM2.

To each detected event we attached a weight w equal to the reciprocal of the detection efficiency of the event. The detection efficiency of the event was assumed to be equal to $\epsilon_\Omega \epsilon_i$, where ϵ_Ω is the probability that the neutron emitted isotropically in the c.m. system is emitted in the direction of the scintillator, and ϵ_i is the probability that this neutron is detected by the scintillator.

As a result of the large angular aperture of the fission and neutron detectors, the determination of both $E_{c.m.}$, the neutron energy in the c.m. system, and of ϵ_Ω are not straightforward. For the purpose of obtaining these quantities, a Monte Carlo simulation of the experiment was carried out. In this simulation the average value of the kinetic energy of the neutron in the lab system, \bar{E}_{lab} , and ϵ_Ω were obtained for sets of values of $E_{c.m.}$ and E_F/A – the kinetic energy of the fission fragment divided by its mass. By carrying out this procedure we solved the inverse problem to the one encountered in the experiment, i.e., in the experiment E_{lab} and E_F/A are measured, while in the calculations $E_{c.m.}$ and E_F/A are given and E_{lab} is derived.

The effective detection efficiency ϵ_i as a function of the time-of-flight channel was obtained here by comparing the binary-fission neutron spectrum of Bowman *et al.*¹¹ (adjusted to our experimental geometry) with our results for neutron emission in binary fission. We define by N_i the number of neutrons per fission event in the time-of-flight channel i of the adjusted binary-fission neutron spectrum of Bowman *et al.*¹¹ Let C_i denote the experimentally determined number of neutrons in channel i per binary-fission event in our experiment. It follows that

$$\epsilon_i = C_i / N_i. \quad (2)$$

The values of ϵ_i thus determined are presented in Fig. 2. The detection efficiency is at first observed to decrease as the energy of the neutron increases and then increases rapidly. The proximity of the scattering chamber to the scintillator in the present experiment enhances the effect of the scattered radiation which appears in both the high- and low-energy regions. At the high-energy end of the spectrum this is mainly due to γ rays emitted in $(n, n'\gamma)$ and (n, γ) reactions, whereas at the low-energy end the scattering is mainly due to (n, n') reactions. The sharp increase in the effective efficiency at high velocities is probably also due to the insufficient separation of γ rays and high-energy neutrons. Similar behavior of the effective efficiency curve in the high-velocity region was

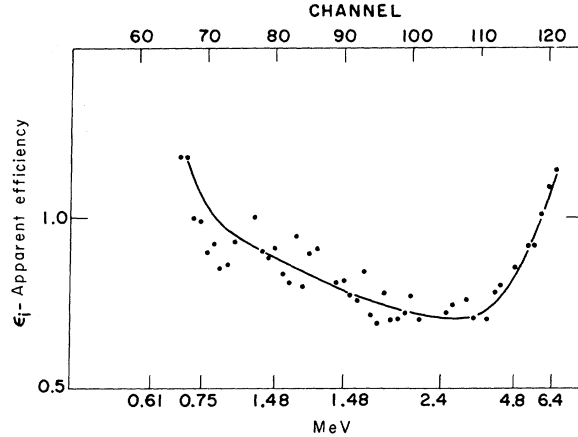


FIG. 2. The effective neutron detection efficiency ϵ_i of the scintillator, as a function of neutron energy and channel number in the TAC spectrum.

observed by Milton and Fraser¹². It should be pointed out that because of the effect of the scattered radiation on the effective detection efficiency, the value of ϵ_i is dependent on the nature of the prompt radiation of the mode of fission being studied. Hence the actual value of ϵ_i may be somewhat different for different mass values of the fission fragments.

IV. RESULTS

A. Properties of the Neutrons

The average number of neutrons emitted per fission event in LRA fission was obtained separately for each neutron counter. The result averaged over both counters is given by

$$\bar{\nu}_{LRA} = 3.11 \pm 0.05.$$

The error quoted is the statistical error only. Let $\bar{\nu}_B$ denote the average number of neutrons in binary fission. We assume here that $\bar{\nu}_B = 3.71$.¹³

$$\bar{\nu}_B - \bar{\nu}_{LRA} = 0.60 \pm 0.05.$$

Piekartz *et al.*¹⁰ obtained recently $\bar{\nu}_B - \bar{\nu}_{LRA} = 0.69 \pm 0.06$ for the spontaneous fission of ^{252}Cf , which agrees within experimental error with our results. Apalin *et al.*¹⁴ obtained $\bar{\nu}_B - \bar{\nu}_{LRA} = 0.68 \pm 0.09$ for the thermal fission of ^{235}U , while Ivanov *et al.*¹⁵ obtained 0.69 ± 0.06 for ^{235}U thermal fission. Hence in both ^{252}Cf and ^{235}U the absolute decrease in the average number of neutrons in LRA as compared with binary fission is the same within the experimental error. However, Adamov *et al.*¹⁶ obtained for ^{244}Cm $\bar{\nu}_B - \bar{\nu}_{LRA} = 1.2 \pm 0.2$, which does not agree with the above quoted results.

The average number of neutrons as a function of fragment mass obtained by us in LRA fission was shown in Ref. 5 together with our result for binary fission. In addition, the values of $\partial\bar{\nu}/\partial E_k$ as a function of fragment mass in both binary and LRA fission were also given in Ref. 5.

The values of $\bar{E}_{c.m.}(A)$ in LRA fission are plotted for comparison with those of binary fission in Fig. 3. The errors in the data are the statistical errors only. In this case, as in the case of the other properties of the neutrons studied in this experiment, the great similarity in the properties of LRA in comparison with binary fission is evident.

The difference in the value of the weighted average of $\bar{E}_{c.m.}$ over all the fission fragment masses for LRA and binary fission is

$$\langle \bar{E}_{c.m.} \rangle_{LRA} - \langle \bar{E}_{c.m.} \rangle_B = 0.05 \pm 0.02 \text{ MeV.}$$

The error quoted here is the statistical error, since the error in the neutron flight path length cancels. This result does not agree with the empirical relation between $\bar{E}_{c.m.}$ and $\bar{\nu}$ derived by Terrell¹ on the basis of the results of a large number of fissioning nuclei. This relation is given by $\bar{E}_{c.m.} = 0.65 \sqrt{\bar{\nu} + 1} \text{ MeV}$, and according to this formula we should have obtained $\langle \bar{E}_{c.m.} \rangle_{LRA} - \langle \bar{E}_{c.m.} \rangle_B = -0.09 \text{ MeV}$.

B. Properties of the Fission Fragments

In Sec. III, it was pointed out that in order to obtain the pre-neutron-emission mass and kinetic energy distributions of the fission fragments, the values of $\bar{\nu}(A)$, the average number of emitted neutrons as a function of fragment mass, must be known. Using the $\bar{\nu}(A)$ values for LRA fission obtained in this experiment, we obtained the mass and energy distributions in LRA fission prior to neutron emission. The total kinetic energy distri-

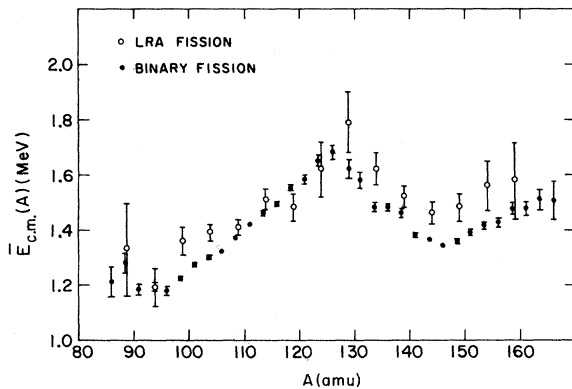


FIG. 3. The average kinetic energy of the neutrons in the c.m. system in binary and LRA fission.

bution and the mass distribution of the heavy- and light-fragment groups were fitted to Gaussian distributions. The most probable values and standard deviations of the fits for binary and LRA fission are given in Table I. The directly calculated average total kinetic energies are also given in the table. All results in the table are pre-neutron-emission values.

The difference between binary and LRA fission in the most probable values of the kinetic energies obtained from the Gaussian fit is

$$\bar{E}_{KB} - \bar{E}_{K LRA} = 12.8 \pm 0.1 \text{ MeV.}$$

The directly calculated average values of E_K give the same result. A difference of $12.1 \pm 0.1 \text{ MeV}$ was obtained by Fraenkel³ for the post-neutron-emission values of \bar{E}_K . Since the fragments lose on the average 0.6 more neutrons in binary fission than in LRA fission, the post-neutron-emission value of $\bar{E}_{KB} - \bar{E}_{K LRA}$ will be lower by about 0.5 MeV than in the pre-neutron-emission value. Hence, the value of $\bar{E}_{KB} - \bar{E}_{K LRA}$ obtained by Fraenkel corrected to pre-neutron-emission fission is $12.6 \pm 0.1 \text{ MeV}$ in comparison with $12.8 \pm 0.1 \text{ MeV}$ obtained here.

The distributions of the total kinetic energy and of the mass groups are observed to be narrower in LRA fission than in binary fission. This has also been pointed out previously by Fraenkel.³

The LRA and binary-fission pre-neutron-emission mass distributions are seen in Fig. 4. The curves are normalized to each other at their peak values. A distinct feature of Fig. 4 is the almost complete overlap of the mass distributions for fragments in the region $130 \leq A \leq 140$. For $94 \leq A \leq 109$ a shift of about half an amu towards lower masses is seen in the LRA curve as compared to

TABLE I. Properties of the fission fragments in LRA and binary fission prior to neutron emission. \bar{E}_K and σ_{E_K} are the most probable values and standard deviation of the total fragment kinetic energy prior to neutron emission. M_L and M_H are the heavy- and light-fragment masses before neutron emission. All values, with the exception of $\langle E_K \rangle$, were obtained from Gaussian fits; $\langle E_K \rangle$ is the average value of E_K .

Experimental values	Binary fission	LRA fission
\bar{E}_K	187.5 \pm 0.1 (MeV)	174.6 \pm 0.1 (MeV)
σ_{E_K}	10.8 \pm 0.1 (MeV)	9.8 \pm 0.06 (MeV)
\bar{M}_L	108.7 \pm 0.1 (amu)	105.9 \pm 0.1 (amu)
σ_{M_L}	6.91 \pm 0.12 (amu)	6.08 \pm 0.08 (amu)
\bar{M}_H	143.3 \pm 0.1 (amu)	142.1 \pm 0.1 (amu)
σ_{M_H}	6.91 \pm 0.12 (amu)	6.08 \pm 0.08 (amu)
$\langle E_K \rangle$	187.3 (MeV)	174.5 (MeV)

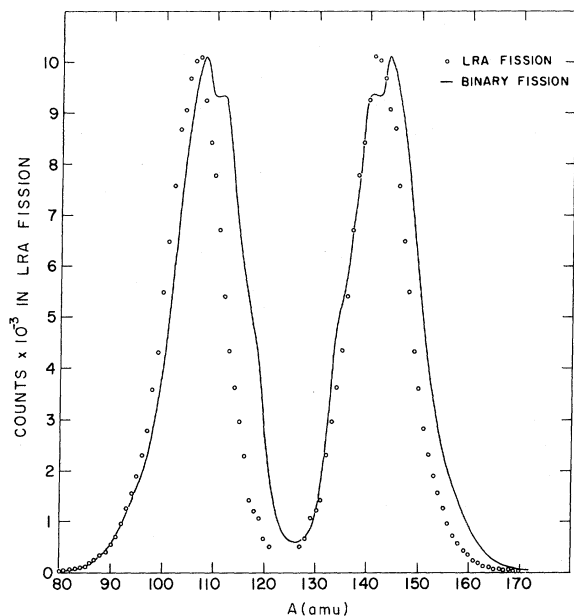


FIG. 4. Pre-neutron-emission fragment mass distribution for binary and LRA fission. The curves were normalized to each other at their peak values.

the binary-fission curve. Schmitt *et al.*,¹⁷ obtained the mass distributions in the LRA and binary fission of $^{236}\text{U}^*$ and plotted their results as in Fig. 4. However, the mass distributions were derived by these authors without taking into account prompt-neutron emission. Their results indicated that in addition to the mass region $130 \leq A \leq 140$, the mass distribution curves overlap in the region $80 \leq A \leq 90$. The latter region corresponds to $94 \leq A \leq 104$ in the ^{252}Cf experiment. In this region we obtained the result that the LRA curve is shifted by about half a mass unit with respect to the binary-fission curve.

It is of interest to note that the binary-fission mass distribution curve obtained here has the same peak structure as the fairly recent time-of-flight results of Bennett and Stein.¹⁸

C. Number of Neutrons as a Function of α -Particle Energy

The average number of neutrons emitted per fission event as a function of α -particle energy, is plotted in Fig. 5. The errors in the graph indicate the statistical errors only. A weighted least-squares fit to a straight line of $\bar{\nu}$ as a function of E_α was carried out and is also plotted in Fig. 5. The slope of this line is given by $d\bar{\nu}/dE_\alpha = -0.026 \pm 0.015 \text{ MeV}^{-1}$. Piekartz *et al.*¹⁰ obtained a value of $-0.045 \pm 0.010 \text{ MeV}^{-1}$ for this slope. Although this result is larger than ours, both values agree within their errors. Apalin *et al.*¹⁴ measured the average number of neutrons per fission

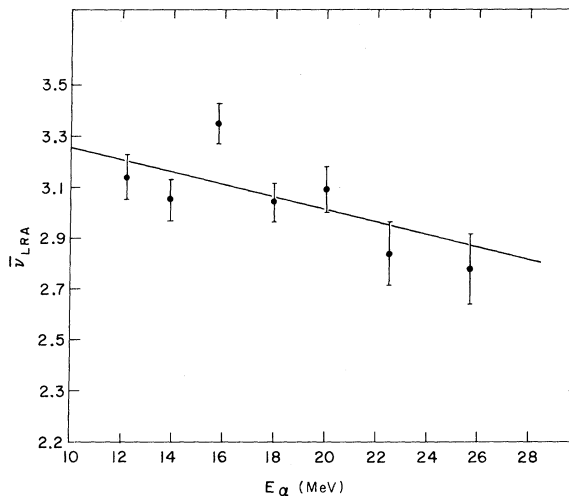


FIG. 5. The average number of neutrons as a function of α -particle energy.

for α particles of energy greater than 22 MeV in the thermal-neutron fission of ^{235}U and obtained a value of $\bar{\nu} = 1.79 \pm 0.13$. This is to be compared with the value of $\bar{\nu} = 1.77 \pm 0.09$ obtained by these authors for all α particles. Our result, which indicates a weak dependence of $\bar{\nu}_{\text{LRA}}$ on E_α , also agrees within experimental error with the results of Apalin *et al.*¹⁴ Adamov *et al.*¹⁶ obtained for ^{244}Cm a slope of 0.08 MeV^{-1} which is substantially larger than the above quoted results.

It is of interest to obtain the correlation of the average excitation energy \bar{E}^* of the fission fragments and the α -particle energy. This correlation may be expressed in the form of $d\bar{E}^*/dE_\alpha$. It may be obtained from the expression

$$\frac{d\bar{E}^*}{dE_\alpha} = \frac{d\bar{\nu}}{dE_\alpha} \frac{dE_K}{d\bar{\nu}} \frac{d\bar{E}^*}{dE_K} \quad (3)$$

The average values in the above equation are averages over both E_K and E_α . $dE_K/d\bar{\nu}$ and $d\bar{E}^*/dE_K$ are also weighted averages over all mass ratios. ($d\bar{E}^*/dE_\alpha$ and $d\bar{\nu}/dE_\alpha$ are assumed to be independent of the mass ratio.) The value of $d\bar{\nu}/dE_K$ was found to be $-0.092 \pm 0.011 \text{ MeV}^{-1}$ for LRA fission.⁵ $d\bar{E}^*/dE_K$ has not been measured, but clearly $|d\bar{E}^*/dE_K| \leq 1$. We thus obtain for $d\bar{E}^*/dE_\alpha$

$$\left| \frac{d\bar{E}^*}{dE_\alpha} \right| \leq (-0.026 \pm 0.015)(-10.9 \pm 1.3)$$

$$= 0.28 \pm 0.19.$$

The above value is to be compared with the result obtained by Fraenkel³ for the correlation be-

tween the average fragment kinetic energy and the α -particle energy $|d\bar{E}_K/dE_\alpha| \approx 0.45$. We see that within experimental error the two quantities are of similar magnitude. Yet there is an indication that $|d\bar{E}_K/dE_\alpha| > |d\bar{E}^*/dE_\alpha|$. Qualitatively this may indicate that α -particle emission in fission occurs to a larger extent at the "expense" of the fragment *kinetic* energy rather than at the "expense" of the fragment *excitation* energy. Moreover, it has been shown above that the difference in the total kinetic energy of the fragments (12.8 MeV) is equal to twice the difference in the excitation energy of binary and LRA fission (5.9 MeV).

The values of $\nu_{\text{LRA}}(A)$ for $E_\alpha < 20$ MeV and for $E_\alpha > 20$ MeV are plotted for comparison in Fig. 6. The curve for $E_\alpha < 20$ MeV looks somewhat flatter than that for $E_\alpha > 20$ MeV, especially in the region of the light masses. However, this may be the result of the larger mass dispersion in the $E_\alpha > 20$ -MeV curve.

V. DISCUSSION

A. Similarity Between Binary and LRA Fission

The similarity of the scission configuration of binary and LRA fission was pointed out previously in Ref. 5. The curves $\bar{\nu}(A)$ and $(\partial\bar{\nu}/\partial E_K)_A$ for binary and LRA fission [Figs. 2(a), 2(b) of Ref. 5] indicated that the behavior of the deformation energy of the fission fragment as a function of fragment mass and fragment kinetic energy is very nearly the same for binary and LRA fission. Hence we concluded that the properties of the scission configuration in both these processes are very similar.

It may be added here that in addition to $\bar{\nu}(A)$ and $(\partial\bar{\nu}/\partial E_K)_A$, the average value, $\bar{E}_{\text{c.m.}}(A)$, of the kinetic energy of the neutrons in the c.m. system as a function of A is nearly equal in binary and LRA fission. This result is not surprising, since $\bar{E}_{\text{c.m.}}(A)$ depends mostly on $\bar{\nu}(A)$ and on the level

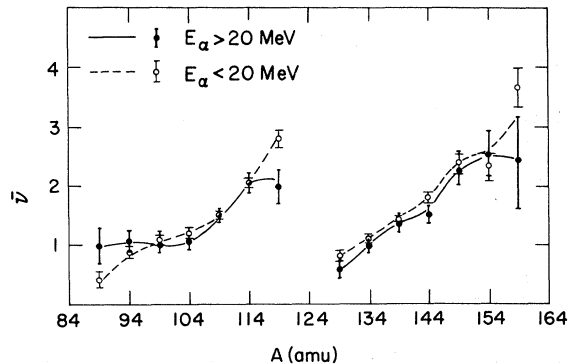


FIG. 6. The average number of neutrons as a function of fragment mass for $E_\alpha < 20$ MeV and for $E_\alpha > 20$ MeV.

density of fission fragments.

The experiments of Piekartz *et al.*¹⁰ with ²⁵²Cf and of Ivanov *et al.*¹⁵ with ²³⁶U are additional proof that the properties of neutrons in LRA and binary fission are very similar. In these experiments the angular distributions of the neutrons were found to be essentially the same in binary and LRA fission. We should also mention the similarity in the properties of the fission fragments in binary and LRA fission³ (i.e., the mass distribution and fragment kinetic energy distribution).

It is of interest to compare the average total prompt energy release, \bar{E}_{TOTAL} of binary and LRA fission. The difference of \bar{E}_{TOTAL} between binary and LRA fission is assumed to be given by

$$\begin{aligned} \bar{E}_{\text{TOTAL}}(\text{BINARY}) - \bar{E}_{\text{TOTAL}}(\text{LRA}) \\ = \Delta\bar{E}_k + \Delta\bar{E}_n + \Delta\bar{E}_\gamma - \bar{E}_\alpha. \end{aligned} \quad (4)$$

$\Delta\bar{E}_k$ is the difference in the average total kinetic energy of the fission fragments in binary and LRA fission. According to the table, the measured value of $\Delta\bar{E}_k$ was found to be 12.9 ± 0.1 MeV for α particles of energy greater than 11.5 MeV. Owing to the negative correlation between the average fragment kinetic energy and α -particle energy, the exclusion of the low-energy α particles causes the measured value of the average fragment kinetic energy to be lower than this value for all the α particles. Fraenkel,³ as pointed out above, obtained $d\bar{E}_K/dE_\alpha = -0.45$. We assume this result to be correct throughout the entire energy region of the α -particle energy spectrum. We also assume that the α spectrum has a Gaussian shape with the values of the most probable energy and standard deviation obtained by Cosper, Cerny, and Gatti.¹⁹ On the basis of these assumptions, the value of \bar{E}_K in LRA fission for all α particles is higher by 0.4 MeV than that measured in this experiment, and we obtain $\Delta\bar{E}_k = 12.5 \pm 0.1$ MeV.

$\Delta\bar{E}_n$ denotes the average energy difference associated with neutron emission. This value is assumed to be given by the equation

$$\Delta\bar{E}_n \equiv (d\bar{\nu}/dE_K)^{-1}(\bar{\nu}_B - \bar{\nu}_{\text{LRA}}). \quad (5)$$

We assume that the $(d\bar{\nu}/dE_K)^{-1}$ is equal to its average value between binary and LRA fission,⁶ i.e., 9.9 MeV. Therefore, $\Delta\bar{E}_n = 5.9 \pm 0.6$ MeV. Owing to the weak dependence of $\bar{\nu}_{\text{LRA}}$ on E_α , the exclusion of the low-energy α particles has a negligible effect on $\Delta\bar{E}_n$; hence $\Delta\bar{E}_n$ is as quoted above.

$\Delta \bar{E}_\gamma$ denotes the average energy change associated with γ -ray emission. No experimental information is available at this stage on $\Delta \bar{E}_\gamma$. We assume here that $\Delta \bar{E}_\gamma = 0$. \bar{E}_α is the average α energy and was obtained from the experimental data of Cospér, Cerny, and Gatti.¹⁹ These authors obtained $\bar{E}_\alpha = 16.0 \pm 0.2$ MeV. Therefore,

$$\bar{E}_{\text{TOTAL}}(\text{BINARY}) - \bar{E}_{\text{TOTAL}}(\text{LRA}) = 2.4 \pm 0.5 \text{ MeV.}$$

We obtain a slightly higher total prompt energy release in binary fission than in LRA fission.

B. α -Particle Emission as a Function of the Mass Ratio

The problem of α -particle emission as a function of the mass ratio has previously been discussed by Schmitt and Feather²⁰ and by Halpern.² The behavior of the α -particle-emission probability $P_\alpha(A_H/A_L)$ as a function of the mass ratio de-

pends critically on the assumption made with regard to the number $x(A)$ of nucleons given up by each fragment in the process of α emission. This statement is supported by the different $P_\alpha(A_H/A_L)$ values obtained by Schmitt and Feather²⁰ and by Halpern² who made different assumptions with regard to the value of $x(A)$.

In order to obtain $P_\alpha(A_H/A_L)$, we assumed that $x(A)$ satisfies the equation

$$x(A) = C[\bar{\nu}_B(A) - \bar{\nu}_{\text{LRA}}(A-x)], \quad (6)$$

i.e., the reduction in the number of neutrons emitted from a fragment of mass A is proportional to $x(A)$. The normalization constant C is equal to $C = 4(\bar{\nu}_B - \bar{\nu}_{\text{LRA}})^{-1} = (0.15)^{-1}$. The same assumption was made by Pick-Pichak.²¹ In order to solve the above equation for $x(A)$ we assume in Fig. 7 four different functional relationships for $x(A)$ and determine which of them best satisfies the equation. In

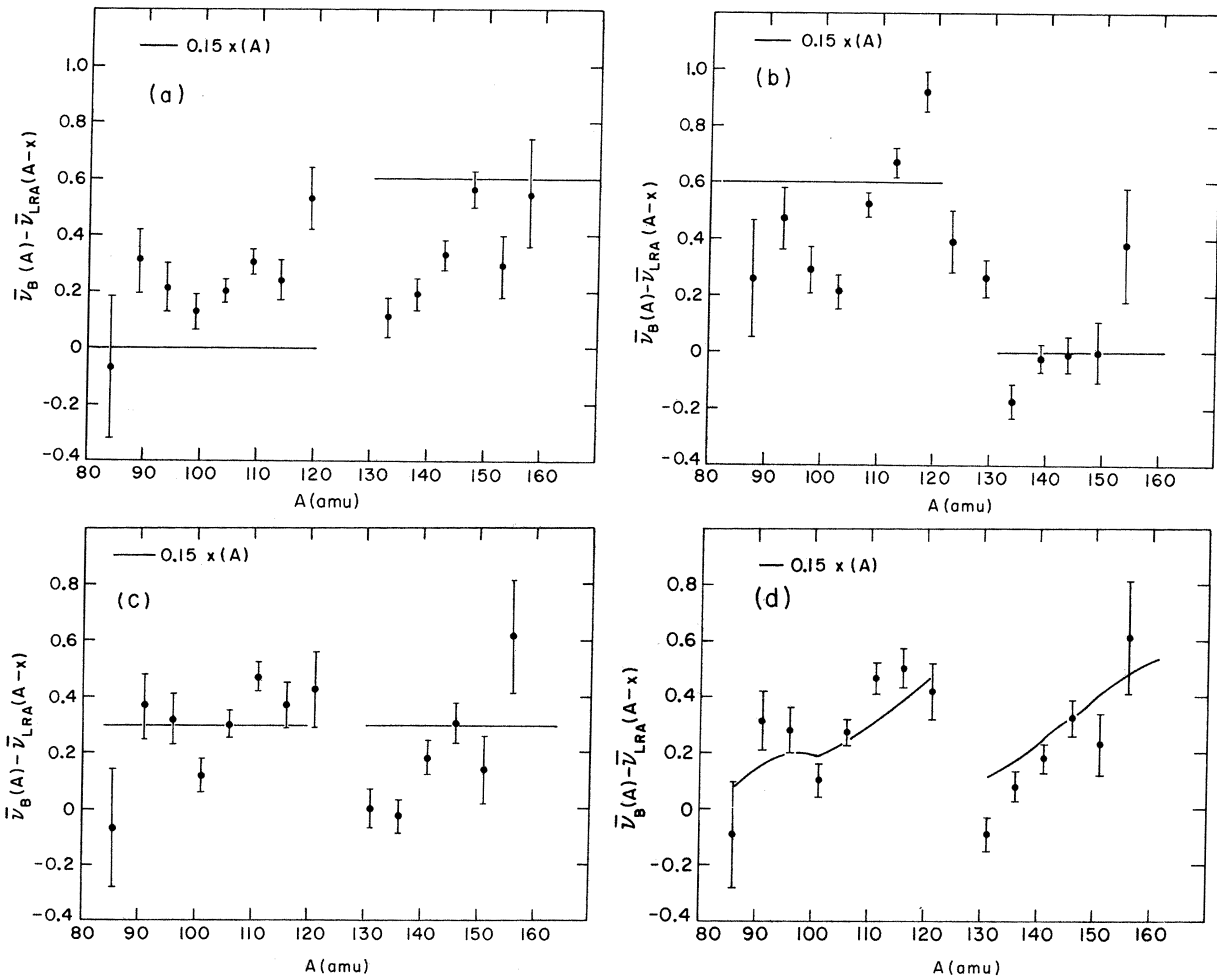


FIG. 7. $\bar{\nu}_B(A) - \bar{\nu}_{\text{LRA}}(A-x)$ for different assumptions regarding the value x . In Fig. 7(a) $x=0$ for $A < 126$ and $x=4$ for $A > 126$; in Fig. 7(b) $x=4$ for $A < 126$ and $x=0$ for $A > 126$; in Fig. 7(c) $x=2$ for all A ; and in Fig. 7(d) $x=4\nu_A/(\bar{\nu}_A + \bar{\nu}_{252-A})$, where $\bar{\nu}_A$ is the average number of neutrons emitted by the fragment A .

(a), we assume $x=4$ for $A > 126$ and $x=0$ for $A < 126$; i.e., the α particle is emitted at the "expense" of the heavy fragment only. In (b), we make the opposite assumption, namely, that α -particle emission occurs at the expense of the light fragment only, i.e., $x=4$ for $A < 126$ and $x=0$ for $A > 126$. In (c), we assume x to be independent of A , namely, $x=2$ for all A . Finally in (d), we assume that for a given mass ratio A_H/A_L we have $x(A_H)/x(A_L) = \bar{\nu}(A_H)/\bar{\nu}(A_L)$, i.e., x is proportional to the relative amount of (original) excitation energy of each fragment of the pair (A_H, A_L) . This may also be written in the form $x(A) = 4\bar{\nu}(A)/[\bar{\nu}(A) + \bar{\nu}(252-A)]$.

In Fig. 7, we compare each of the four assumptions for $C^{-1}x(A)$ with the curve $\bar{\nu}_B(A) - \bar{\nu}_{LRA}(A-x)$. It is seen that assumption (d) gives the best agreement with the equation $C^{-1}x(A) = [\bar{\nu}_B(A) - \bar{\nu}_{LRA}(A-x)]$. Hence we may conclude that $x(A) = 4\bar{\nu}(A)/[\bar{\nu}(A) + \bar{\nu}(252-A)]$. We denote by $Y_B(A)$ and $Y_{LRA}(A)$ the fragment mass yields in binary and LRA fission. We have

$$P_\alpha(A_H, A_L) = \frac{Y_{LRA}(A_H - x_H)}{Y_B(A_H)} = \frac{Y_{LRA}(A_L - x_L)}{Y_B(A_L)}, \quad (7)$$

where x_H is the number of nucleons given up by the heavy fragment. We show in Fig. 8 the function $P_\alpha(A_H, A_L)$, using relationship (d) above for $x(A)$. $P_\alpha(A_H, A_L)$ is normalized to 1 for $A_H = 145$. It is observed that P_α is almost independent of the mass ratio. Our results differ from those of both Schmitt and Feather²⁰ and Halpern² who both found a strong dependence of P_α on the mass ratio.

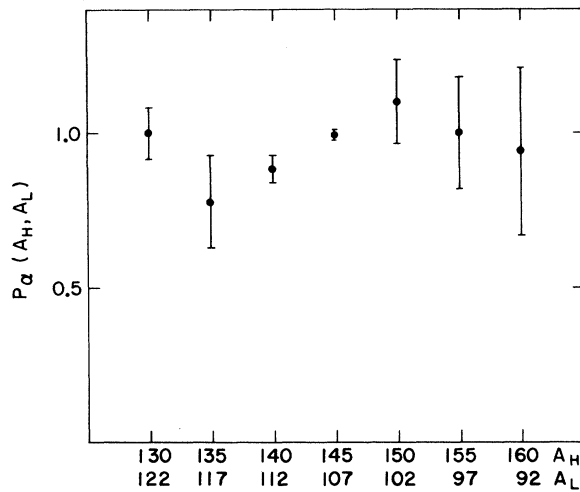


FIG. 8. The relative emission probability of the α particle as a function of the mass value of the fission fragments.

APPENDIX. EVALUATION OF ERRORS IN THE TIME OF FLIGHT OF THE NEUTRONS AND IN THE NEUTRON ENERGY IN THE LABORATORY AND CENTER-OF-MASS SYSTEMS

One source of error in the evaluation of the time of flight of the neutron is the relatively large depth of the scintillator compared to the total flight path. For a neutron incident on the scintillator at a given angle the standard deviation σ_T of the time of flight T was calculated using the method of Bowman *et al.*¹¹ (The interaction was assumed to be with the protons of the scintillator only.) It was found that $\sigma_T/\bar{T} \cong 0.08$ for 2-MeV neutrons and is only weakly dependent on E_{lab} .

Because of the relatively large angular aperture of the neutron counter in the present experiment, the angle θ between the direction of the neutron and the axis of the detector could assume values between 0 and 12°. The Monte Carlo calculations show that for the different pairs of E_F/A and $E_{c.m.}$, the mean value of the angle θ is relatively constant and is close to 7°. For a given set of E_F/A and $E_{c.m.}$, the value of σ_θ is of the order of not more than 2.5°. Thus the large angular aperture does not affect the uncertainty in the flight path by more than 1%, and is negligible compared with the dispersion due to the large scintillator depth.

Another source of uncertainty in the time-of-flight value is the experimental time resolution, the standard deviation of which was equal to 1.5 nsec. ΔT , the total standard deviation in the measurement of \bar{T} , is given by

$$\Delta T/\bar{T} = [\sigma_T^2/\bar{T}^2 + (1.5)^2/\bar{T}^2]^{1/2}. \quad (A1)$$

For a 2.0-MeV neutron, $\Delta T/\bar{T} = 0.11$. The experimental error in the determination of E_{lab} is given by $2\Delta T/\bar{T}$. As was discussed above, the relation between E_{lab} and E_F/A and $E_{c.m.}$ was obtained by means of the Monte Carlo calculation. $E_{c.m.}$ was then obtained from this calculated relation and the experimental values of E_{lab} and E_F/A . However, the Monte Carlo calculation does not yield a unique value of E_{lab} for a given set of E_F/A and $E_{c.m.}$ but rather a distribution. The standard deviation of this distribution is denoted by δE_{lab} . The standard deviation $\Delta E_{c.m.}$ of $E_{c.m.}$ is thus due to both the uncertainty δE_{lab} in E_{lab} and to the experimental error in E_{lab} resulting from the error in the time-of-flight value T [see Eq. (A1)]. It was found for the various E_F/A and $E_{c.m.}$ values that $\Delta E_{c.m.}/\bar{E}_{c.m.} \cong 0.23$.

The neutron spectrum in the c.m. system expressed as a function of the energy over the average c.m. energy can be described by a standard

function⁹ for the different fragment masses. The standard deviation of this spectrum is denoted by $\sigma_{E_{c,m}}$, and $\sigma_{E_{c,m}}/\bar{E}_{c,m} = 0.82$.⁹ Hence the dispersion due to the experimental error in the mea-

surement of $E_{c,m}$ is less than the width of the spectrum. The effect of the experimental dispersion in the determination of $\bar{E}_{c,m}(A)$ is therefore small.

- ¹J. Terrell, Phys. Rev. 127, 880 (1962).
²I. Halpern, CERN Report No. CERN-6812, 1963 (unpublished); in *Proceedings of the Symposium on the Physics and Chemistry of Fission, Salzburg, Austria, 1965* (International Atomic Energy Agency, Vienna, Austria, 1965), Vol. II, p. 369.
³Z. Fraenkel, Phys. Rev. 156, 1283 (1967).
⁴Y. Boneh, Z. Fraenkel, and I. Nebenzahl, Phys. Rev. 156, 1305 (1967).
⁵E. Nardi and Z. Fraenkel, Phys. Rev. Letters 20, 1248 (1968).
⁶H. W. Schmitt, W. E. Kiker, and C. W. Williams, Phys. Rev. 137, 837 (1965).
⁷S. L. Whetstone, Jr., Phys. Rev. 131, 1232 (1963).
⁸H. W. Schmitt, J. H. Neiler, and F. J. Walter, Phys. Rev. 141, 1146 (1966).
⁹H. R. Bowman, J. C. D. Milton, S. G. Thompson, and W. J. Swiatecki, Phys. Rev. 129, 2133 (1963).
¹⁰H. Piekartz, J. Blocki, T. Krogulski, and E. Piasecki, Nucl. Phys. A146, 273 (1970).
¹¹H. R. Bowman, S. G. Thompson, J. C. D. Milton, and W. J. Swiatecki, Phys. Rev. 126, 2120 (1963).
¹²J. C. D. Milton and J. S. Fraser, in *Proceedings of the Symposium on the Physics and Chemistry of Fission, Salzburg, Austria, 1965* (International Atomic Energy Agency, Vienna, Austria, 1965), Vol. II, p.39.
¹³D. W. Colvin and M. G. Sowbery, in *Proceedings of the Symposium on the Physics and Chemistry of Fission, Salzburg, Austria, 1965* (International Atomic Energy Agency, Vienna, Austria, 1965), Vol. II, p. 25.
¹⁴V. F. Apalin, Y. P. Dobrynin, V. P. Zakharova, I. E. Kutikov, and L. A. Mikaelyan, J. Nucl. Energy 13, 85 (1961).
¹⁵O. I. Ivanov, N. I. Kroshkin, V. N. Netedov, and V. P. Kharin, Yadern. Fiz. 5, 737 (1967) [transl.: Soviet J. Nucl. Phys. 5, 523 (1967)].
¹⁶V. M. Adamov, L. V. Drapchinskii, S. S. Kovalenko, K. A. Petrzhak, and I. I. Tutugin, Yadern. Fiz. 5, 52 (1967) [transl.: Soviet J. Nucl. Phys. 5, 30 (1967)].
¹⁷H. W. Schmitt, J. H. Neiler, F. J. Walter, and A. Chetham-Strode, Phys. Rev. Letters 9, 427 (1962).
¹⁸M. J. Bennett and W. E. Stein, Phys. Rev. 156, 1277 (1967).
¹⁹S. W. Cospers, J. Cerny, and R. C. Gatti, Phys. Rev. 154, 1193 (1967).
²⁰H. W. Schmitt and N. Feather, Phys. Rev. 134, B565 (1965).
²¹G. A. Pick-Pichak, Yadern. Fiz. 4, 1147 (1966) [transl.: Soviet J. Nucl. Phys. 4, 826 (1967)].